Static and rotating domain-wall cross patterns in Bose-Einstein condensates

Boris A. Malomed,[1] H. E. Nistazakis,[2] D. J. Frantzeskakis,[2] and P. G. Kevrekidis[3]
[1]*Department of Interdisciplinary Studies, Faculty of Engineering, Tel Aviv University, Tel Aviv 69978, Israel*
[2]*Department of Physics, University of Athens, Panepistimiopolis, Zografos, Athens 15784, Greece*
[3]*Department of Mathematics and Statistics, University of Massachusetts, Amherst, Massachusetts 01003-4515, USA*
(Received 13 May 2004; published 18 October 2004)

For a Bose-Einstein condensate (BEC) in a two-dimensional (2D) trap, we introduce cross patterns, which are generated by the intersection of two domain walls (DWs) separating immiscible species, with opposite signs of the wave functions in each pair of sectors filled by the same species. The cross pattern remains stable up to the zero value of the immiscibility parameter $|\Delta|$, while simpler rectilinear (quasi-1D) DWs exist only for values of $|\Delta|$ essentially exceeding those in BEC mixtures (two spin states of the same isotope) currently available to the experiment. Both symmetric and asymmetric cross configurations are investigated, with equal or different numbers $N_{1,2}$ of atoms in the two species. In rotating traps, "propellers" (stable revolving crosses) are found too. A full stability region for the crosses and propellers in the system's parameter space is identified, unstable crosses evolving into arrays of vortex-antivortex pairs. Stable rotating rectilinear DWs are found too, at larger values of $|\Delta|$. All the patterns produced by the intersection of three or more DWs are unstable, rearranging themselves into ones with two DWs. Optical "propellers" are also predicted in a twisted nonlinear photonic-crystal fiber carrying two different wavelengths or circular polarizations, which can be used for applications to switching and routing.

DOI: 10.1103/PhysRevA.70.043616 PACS number(s): 03.75.Mn, 03.75.Kk, 03.75.Lm, 89.75.Kd

I. INTRODUCTION

Domain walls (DWs) separating immiscible species are generic dynamical structures in mixed Bose-Einstein condensates (BECs) [1]. Originally, the DWs were studied in one-dimensional (1D) BEC models, but they can be naturally extended into the 2D geometry as quasi-1D objects [2,3]; in particular, circular DWs, between a less repulsive component in the middle of the trap and a more repulsive one forming an outer shell, have been found. Recently, complex 2D large-area structures in rotating binary BECs were predicted in simulations, including vortex lattices and sheets in mixtures [4,5].

Our aim is to construct genuinely two-dimensional DW patterns, in the form of *crosses* formed by the intersection of two DWs, in trapped binary BECs. We will consider both symmetric and asymmetric crosses, depending on the ratio of the numbers of atoms in the two species ("stoichiometric ratio"). Patterns in a rotating trap will be considered too. A rotating DW cross seems like a "double-vane propeller," which may also be symmetric or asymmetric. Note that the DWs may move, in the general case; however, their motion is not amenable to straightforward observation in the 1D settings, because of the relatively small size of domains available in BEC experiments. Thus, the "propeller" offers a unique possibility to create *permanently moving* DWs. We identify stability regions for the quiescent and rotating crosses, and investigate the evolution of unstable ones. All multihanded crosses, formed by the intersection of more than two DWs, are shown to be unstable. We will also briefly consider rotating one-dimensional (rectilinear) DWs, i.e., "single-vane propellers" (however, we conclude that the rectilinear DWs are less relevant than the crosses for experiments with currently available BEC mixtures).

An appealing feature of the cross structures is the feasibility of their experimental realization in binary BECs. Experimental creation of two-component mixtures has already been reported for different spin states in ^{87}Rb [6,7] and ^{23}Na [8]. Accordingly, the use of a mixture of two spin states of the same isotope seems to be the most straightforward way of creating the DW cross configuration, as the latter can be imprinted onto the BEC by optical beams passed through a properly designed phase mask. Moreover, the DW cross appears, in our extensive computations, to be the most robust structure among the various types of domain walls considered. Indeed, the immiscibility condition for the repulsive BEC mixture (the one with positive scattering lengths of atomic collisions) is

$$\Delta \equiv \alpha_{11}\alpha_{22} - \alpha_{12}^2 \leqslant 0, \tag{1}$$

where α_{11}, α_{22}, and α_{12} are strengths of the intraspecies and interspecies interactions, respectively [see Eqs. (5) and (7) below]. As is shown below, the crosses (both static and rotating ones) remain stable up to $|\Delta|=0$, while the rectilinear DW is stable only for

$$\Delta \leqslant \Delta_{\rm rect}^{\rm (cr)} = -0.061. \tag{2}$$

On the other hand, experimental measurements [6,7] yield an extremely small actual value of $|\Delta|$ in the mixture of two spin states of ^{87}Rb,

$$\Delta_{\rm Rb} \approx -0.0009, \tag{3}$$

which *does not* satisfy the condition (2). For the mixture of different spin states in ^{23}Na, the immiscibility parameter extracted from experimental measurements is larger,

$$\Delta_{\rm Na} \approx -0.036 \tag{4}$$

[8], but it does not meet the condition (2) either.

We also note in passing that work is currently in progress towards the creation of two-component BECs with different atomic species, such as ^{41}K:^{87}Rb [9] and ^{7}Li:^{133}Cs [10]. In that case, $|\Delta|$ may take values very different from those given in Eqs. (3) and (4). Furthermore, we should note that an additional possibility to push the experimental values of Δ toward the critical one mentioned above is through the use of the so-called Feshbach resonance [11] that can control the strength of the interatomic interactions.

The same "propeller" effect may be implemented in completely different physical media, namely, photonic crystals (PCs) or photonic-crystal fibers (PCFs), with a self-defocusing nonlinearity and a superimposed twist. In PCFs, the twist bends the inner holes, which run along the fiber, into helices. In that case, the cross configuration may be realized as an intersection of stable optical DWs separating two orthogonal circular polarizations or two different carrier wavelengths (previously, spatial-domain optical DWs between different polarizations were predicted in driven dissipative cavities [12], but no experimental setting was proposed to observe their permanent motion). The twist-induced rotation of the DW cross may take place along the propagation distance, so that the entire pattern will seem like a double helix. Twisted PCs per se were studied in a stack model [13], and very recently the first twisted PCF was fabricated [14] (it was used as a polarization filter). Note that, combining a modulation of the air holes density along the radius of the PCF core and a properly structured cladding, the distribution of the effective refractive index across the PCF can be made similar to the parabolic trapping potential in the BEC model (see below).

Besides the first possibility to observe permanent motion of optical DWs (in the spatial domain), the proposed configuration suggests a design of a new all-optical switch: the turn of the sectors occupied by a signal field, with a specific circular polarization or wavelength, just by 90° is sufficient for complete switching. The diameter of the twist-tolerant PCFs, $\simeq 100$ μm, and their length, a few centimeters (which is tantamount to tens of rotation periods) [14], make these experiments and applications quite feasible. Moreover, the copropagation of several different wavelengths in the PC fiber can make a *stable multi-handed* cross and propeller possible. The latter may be promising for routing applications in wavelength-division-multiplexed (WDM) telecommunications. Similar configurations with more than two species may also be relevant in terms of immiscible multicomponent BEC mixtures. The latter issue will be considered elsewhere.

The paper is organized as follows. In Sec. II, we construct the rectilinear and cross DW configurations and study some of their properties. In Sec. III, we focus on the stability of crosses, including rotating ones. The above-mentioned "single-vane propeller" (a rotating rectilinear DW) is also discussed. Section IV summarizes our findings and presents our conclusions.

II. CONSTRUCTION AND PROPERTIES OF DOMAIN-WALL CONFIGURATIONS

The two-component rotating repulsive BEC is described by a system of coupled Gross-Pitaevskii (GP) equations [15],

$$i\hbar\frac{\partial\psi_j}{\partial t}=\left[\hat{H}+\sum_{k=1,2}g_{jk}|\psi_k|^2\right]\psi_j,\quad j=1,2, \tag{5}$$

where ψ_j are the wave functions of the two species, normalized so that $N_j=\int|\psi_j|^2d\mathbf{r}$ is the respective number of atoms. The single-species Hamiltonian in Eq. (5) is $\hat{H}=-(\hbar^2/2m)\nabla^2-\omega_L\tilde{L}_z+\tilde{V}$, where m is the atomic mass (assuming a mixture of two spin states of the same isotope), ω_L is the rotation frequency, and $\tilde{L}_z=i\hbar(x\partial_y-y\partial_x)$ is the angular-momentum operator. The trapping potential is

$$\tilde{V}=\frac{m}{2}(\omega_r^2r^2+\omega_z^2z^2), \tag{6}$$

where $r^2\equiv x^2+y^2$, and the confining frequencies ω_r and ω_z are assumed to obey the condition $\omega_r/\omega_z\equiv\Omega\ll 1$. The intraspecies and interspecies interactions are characterized by the coefficients $g_{jj}=4\pi\hbar^2a_{jj}/m$ and $g_{12}\equiv g_{21}=4\pi\hbar^2a_{12}/m$, respectively, where a_{jk} are the corresponding scattering lengths; as mentioned above, we consider the (most typical) case of positive a_{jk}. Then, the condition of the immiscibility between the components takes the well-known form of Eq. (1).

Following Ref. [16], effective 2D GP equations can be derived from the 3D ones. To this aim, measuring the coordinates and time in units of the harmonic-oscillator length and period, i.e., $\sqrt{\hbar/m\omega_z}$ and $1/\omega_z$, respectively, we seek solutions to Eqs. (5) as $\psi_j(r,z,t)=(2\pi)^{-1/4}\sqrt{\hbar\omega_z/g_{11}}u_j(r,t)\Phi_j(z)\exp(-i\gamma_jt)$, where $\Phi_j(z)=\pi^{-1/4}\exp(-z^2/2)$ is the ground state of the 1D harmonic oscillator. Multiplying the resulting equations by $\Phi^\star$ and integrating it in z, we arrive at a system of 2D equations,

$$i\frac{\partial u_j}{\partial t}=\left[\hat{H}_{2D}+\sum_{k=1,2}\alpha_{jk}|u_k|^2\right]u_j,\quad j=1,2, \tag{7}$$

$$\hat{H}_{2D}\equiv(-1/2)\nabla_\perp^2+V(r)-\Omega_LL_z, \tag{8}$$

where $\nabla_\perp^2$ is the 2D Laplacian, and

$$V(r)\equiv(1/2)\Omega^2r^2,\quad L_z\equiv i(x\partial_y-y\partial_x),\quad \Omega_L\equiv\omega_L/\omega_z. \tag{9}$$

The nonlinearity coefficients in the 2D system (7) are $\alpha_{11}=1$, $\alpha_{12}=g_{12}/g_{11}$, and $\alpha_{22}=g_{22}/g_{11}$. Then, the numbers of atoms in the species are $N_j=(4\sqrt{2}\pi^{3/2})^{-1}\sqrt{\hbar/m\omega_z}Q_j$, where $Q_j\equiv\int|u_j|^2d^2\mathbf{r}_\perp$ are the norms of the 2D wave functions.

The spatial evolution of bimodal optical beams in the above-mentioned twisted PCFs is also described by Eqs. (7) for the amplitudes u_j of the two components, with t replaced by the propagation distance z, and $V(r)$ in Eq. (8) is a potential function describing the cladding surrounding the PCF proper. In this case, N_j are total powers of the two components of the beam, and the nonlinear coefficients take values close to $\alpha_{12}=2\alpha_{11}=2\alpha_{22}$; according to Eq. (1), the latter values definitely guarantee the "immiscibility" (mutual repulsion of the two optical modes).

Solutions to Eqs. (7) in the form of either a simple rectilinear DW (first, without the rotation, $\Omega_L=0$) are constructed

as follows. We start with the Thomas-Fermi (TF) configuration for the two components with chemical potentials μ_j,

$$(u_j)_{\mathrm{TF}} = e^{-i\mu_j t}\sqrt{[\mu_j - V(r)]/\alpha_{jj}}, \tag{10}$$

if $\mu_j - V(r) > 0$ and $(u_j)_{\mathrm{TF}} = 0$ otherwise (in the PCFs, $-\mu_j$ are the propagation constants of the optical modes). Then, to construct a rectilinear DW, we effectively remove each component from a half-plane, upon multiplying $(u_j)_{\mathrm{TF}}$ by

$$f_j(x) \equiv \frac{1}{2}[1 - (-1)^j \tanh x]. \tag{11}$$

The resulting function $u_1(u_2)$ is positive in the left (right) half of the (x,y) plane.

To construct a DW cross in a similar fashion, we also start from the TF ansatz (10), and then remove two quarter-planes in each component, multiplying the expression (10) by $(1/2)[f_j(x)f_j(y) + f_j(-x)f_j(-y)]$, where the factors $f_{1,2}$ are defined as per Eq. (11). As a result, the wave functions u_1 and u_2 have support, respectively, practically only in the quadrants (sectors) 1 and 3 (i.e., $xy > 0$), and 2 and 4 (i.e., $xy < 0$). Next, we multiply the entire configuration by $(-1)^j \tanh x$, hence the functions u_1 and u_2 are, respectively, positive (negative) in the sectors 1 (3) and 2 (4). In other words, we introduce the phase shift of π between the two quadrants filled by each species (in other words, we aim to construct a DW cross which, simultaneously, is a "latent dark soliton" in each component). Without these phase shifts, the cross will be obviously unstable against splitting into a set of two approximately parallel quasirectilinear DWs, as a pair of the sectors filled by the same species without the phase shift between them will tend to merge into a single stripelike pattern.

After the prototype rectilinear or cross DW configuration was constructed as described above, Eqs. (7) were numerically integrated in imaginary time, to let the system relax into a stable stationary state closest to the prototype one (which is a well-known technical ruse). For the DW-cross case, the relaxation in imaginary time did not essentially alter the prototype pattern, always converging to a numerically exact stable cross pattern, provided that the immiscibility condition (1) was met. This outcome of the imaginary-time integration took place for *arbitrarily small* values of the immiscibility coefficient $|\Delta|$, including the case when Δ was set precisely equal to 0. With $\Delta > 0$, the integration always showed that two species would completely mix into a uniform state.

In the case of the rectilinear DW, the imaginary-time integration converged to a stable quasi-1D DW pattern only if the condition (2) was satisfied, which is more restrictive than the general immiscibility criterion (1). For smaller values of $|\Delta|$, stable rectilinear DWs could never be found; instead, the two species would completely mix up, even if Δ was negative. Thus, the DW-cross pattern, although being more complex than its simplest rectilinear counterpart, is a much more robust one, and has a much better chance to be created in experiments with the currently available *weakly immiscible* spin-state mixtures that actually do not satisfy the condition (2), see Eqs. (3) and (4). The extra robustness of the DW-cross structure may be explained by the additional π phase shifts lent to both its components, as described above.

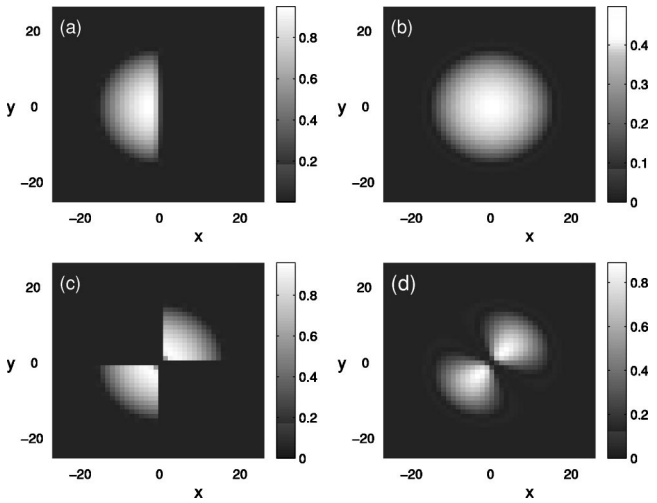

FIG. 1. Gray-scale plots showing the distribution of the density $|u_1|^2$ of one species (the density $|u_2|^2$ is complementary to $|u_1|^2$) in the initial configuration (a) corresponding to the prototype rectilinear DW, and in the corresponding final counterpart (b), which is generated by the numerical integration of the GP equations (7) in imaginary time, in the case of weak immiscibility, with $\Delta = -9 \times 10^{-4}$ (corresponding to $\alpha_{11} = 1$, $\alpha_{22} = 0.94$, $\alpha_{12} = 0.97$) and $\Omega = 0.05$. The panels (c) and (d) display the same for the initial and final configurations in the case of the DW cross.

As an example, in Fig. 1 we show the result of the relaxation for each type of the prototype pattern, with the value of Δ taken as for the spin-state mixture in ^{87}Rb, see Eq. (3). This was realized by setting $\alpha_{11} = 1$, $\alpha_{22} = 0.94$, and $\alpha_{12} = 0.97$ in Eq. (7). As is seen, the rectilinear DW pattern cannot be formed indeed, preferring to mix itself up into a uniform state [panels (a) and (b)]. On the contrary, the initial (prototype) DW-cross pattern readily relaxes into a configuration of exactly the same type.

In the example shown in Fig. 1, the normalized magnetic-trap strength is $\Omega = 0.05$ [see Eq. (9)], and both chemical potentials are set equal to 1. In terms of the real-world parameters, this choice corresponds to a mixture of two spin states in the ^{87}Rb condensate in a disk-shaped trap with

$$\omega_r = 2\pi \times 6 \text{ Hz}, \quad \omega_z = 2\pi \times 120 \text{ Hz} \tag{12}$$

[see Eq. (6)], the initial TF radius and numbers of atoms in each species being

$$R = 34\ \mu\text{m}, \quad N = 3.6 \times 10^3. \tag{13}$$

In what follows below, we will display examples for larger $|\Delta|$, which may be unrealistically large directly (but may be attainable through the use of the Feshbach resonance [11] mentioned above). This allows us to generate patterns that are much sharper and easier to understand, while qualitatively they are completely tantamount to those found at smaller (more directly realizable) values of the immiscibility parameter. So, we will fix

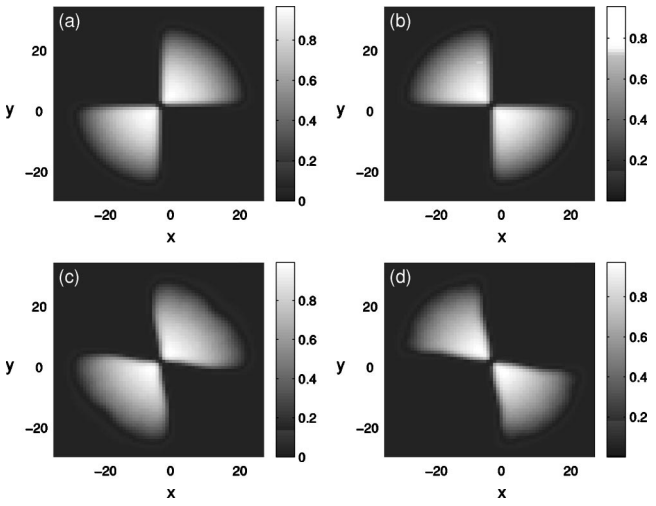

FIG. 2. Gray-scale plots of the densities of the two species, $|u_1|^2$ and $|u_2|^2$ (left and right panels), in the symmetric (a,b) and asymmetric (c,d) DW-cross patterns. The parameters are $\alpha_{11}=1$, $\alpha_{22}=1.01$, $\alpha_{12}=1.52$, and $\Omega=0.05$. In the symmetric configuration, $\mu_1=\mu_2=1$, and in the asymmetric one, $\mu_1=1.1025$, $\mu_2=1$ and $N_1/N_2=1.2$, $\theta_1=6\pi/11$, $\theta_2=5\pi/11$. The estimate (in physical units) for the Thomas-Fermi diameter for both configurations is 68 μm.

$$\alpha_{11}=1, \quad \alpha_{22}=1.01, \quad \alpha_{12}=1.52, \tag{14}$$

which corresponds to $\Delta=-1.3$.

Before proceeding further, it is important to note that, alongside the symmetric DW-cross configurations like the one shown in Fig. 1(d), *asymmetric* ones are possible too, with different numbers of atoms in the two species, $Q_1 \neq Q_2$. Indeed, the TF approximation (10) yields

$$Q_j=\left(\frac{\pi}{2\alpha_{jj}}\right)\left(\mu_j-\frac{1}{4}\Omega^2R^2\right)R^2, \tag{15}$$

where R is the TF radius of the state; consequently, $\alpha_{11} \neq \alpha_{22}$ and/or $\mu_1 \neq \mu_2$ lead to $Q_1 \neq Q_2$, and, as a result, to asymmetric crosses. We have checked that the numerical results always obey a natural relation, $N_1/N_2 \equiv Q_1/Q_2=\theta_1/\theta_2$, where θ_j is the intrinsic angle of the jth sector, with $\theta_1+\theta_2 \equiv \pi$. Examples of the symmetric and asymmetric DW crosses are shown, respectively, in the top and bottom panels of Fig. 2.

III. STABILITY AND ROTATION OF THE DOMAIN-WALL PATTERNS

A. Static domain-wall crosses

Dynamical stability of the symmetric and asymmetric DW crosses is a crucially important issue. We have found that, for a fixed trap's strength Ω, the stability strongly depends on the stoichiometry ratio N_1/N_2, more symmetric configurations being more robust. To show this, we fix the nonlinearity coefficients α_{jj} as in Eqs. (14), set $\mu_2=1$ and, then, for a given value of Ω in the interval $(0,0.25)$, we vary μ_1 to induce variation of the ratio $N_1/N_2 \equiv Q_1/Q_2$, as per Eq. (15). Finally, we simulate Eqs. (7) in real time (up to $t=1000$), to test the stability of the configuration. The resulting stability domain in the $(N_1/N_2,\Omega)$ parametric plane is displayed in Fig. 3(a). For example, at $\Omega=0.05$, which corresponds to the above-mentioned values (12) and (13) of the physical parameters, Fig. 3(a) shows that stable DW crosses exist in the interval $0.65 \leqslant N_1/N_2 \leqslant 1.65$. We note that, alternatively, it is possible to represent the domain of stability of the static DW crosses in the (μ_1,μ_2) plane, for a fixed value of Ω (then, each point of the domain would correspond to a given value of N_1/N_2). This can be done, e.g., upon rescaling the variables in Eqs. (7) and (8) so that $\Omega=1$ (see also a discussion in Sec. III B); in that case, the domain of stability would be a triangular shaped zone enclosing the line $\mu_1=\mu_2$ [17].

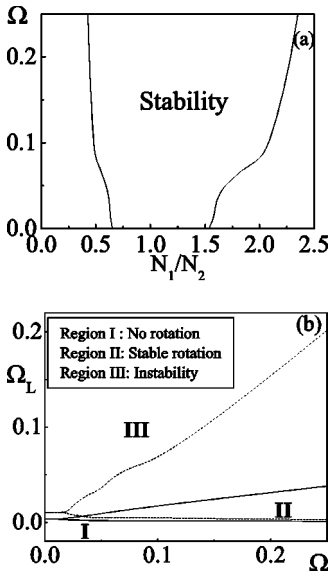

FIG. 3. Stability regions for the static (a) and rotating (b) DW crosses. The values of the nonlinear coefficients are fixed as in Eqs. (14). In (b), solid and dashed lines, respectively, show borders of the stable-rotation region for symmetric and asymmetric crosses (in the latter case, $N_1/N_2=1.5$).

Evolution of unstable DW crosses is also an issue of interest. A typical example of the instability development (in the component with the larger number of atoms) is displayed in Fig. 4 for $\mu_1=1.8025$ and $\mu_2=1$, which corresponds to $N_1/N_2=2.5$. At an initial stage, the cross quickly rearranges into a quasi-1D object, which is actually a dark soliton in the species with the larger number of atoms, coupled to a bright soliton in the other species (this object resembles structures considered in Ref. [3]). The latter configuration is itself subject to a *snaking instability*, which is a known feature of quasi-1D dark solitons in BECs filling 2D areas [18] (we stress that, unlike the dark solitons, the rectilinear DWs are not subject to this instability). The snaking instability initiates a break-up of the dark stripe into four vortex-antivortex pairs in the first species, with the second species collecting itself into spots coupled to the pairs. Finally, the four vortex-antivortex pairs annihilate into two. The latter configuration persists for long times, and it may be related to serpentine-shaped vortex sheets reported in recent 2D simulations of large-size BECs [4]. It would be desirable to analyze this

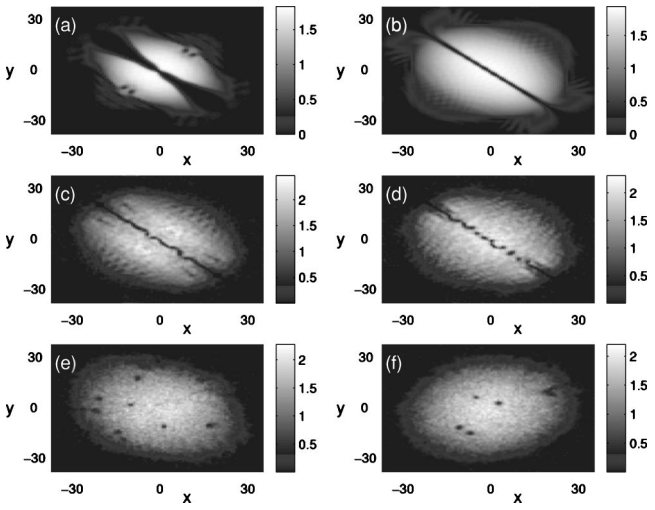

FIG. 4. Evolution of the density $|u_1|^2$ of the species with the larger number of atoms in an unstable DW cross, for the same parameters as in Fig. 2, but with $\mu_1=1.8025$. In this case, $N_1/N_2=2.5$ and $\theta_1=5\pi/7$, $\theta_2=2\pi/7$. The snapshots (a)–(f) correspond to $t=0$, $t=100$, $t=310$, $t=316$, $t=1000$, and $t=2200$, respectively (the physical time unit is 1.33 ms). The density $|u_2|^2$ is complementary to $|u_1|^2$, as in Figs. 2(c) and 2(d).

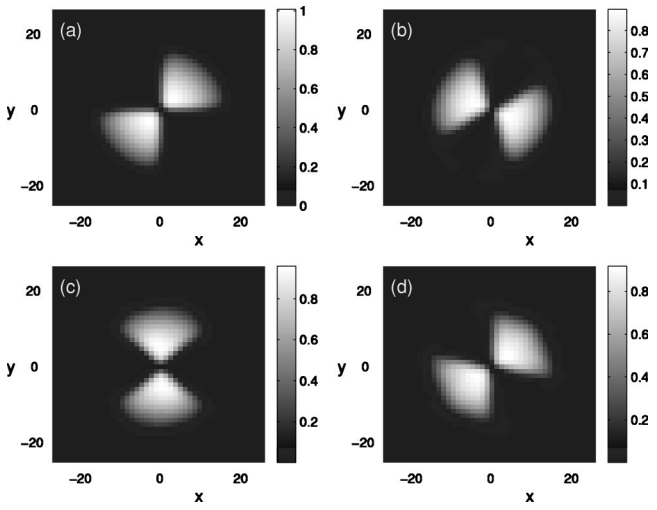

FIG. 5. A stable rotating asymmetric domain-wall cross ("double-vane propeller"). The four snapshots (a), (b), (c), and (d) show the distribution of the density $|u_1|^2$ at consecutive time moments—$t=0$, $T/6$, $T/3$, and $T/2$, respectively—which cover half of the rotation period, $T/2=\pi/\Omega_L\approx 52.3$ ($\simeq$70 ms, in physical units). The parameters are as in Figs. 2(c) and 2(d) but with $\Omega=0.1$ and $\Omega_L=0.06$.

instability by means of a finite-mode stability analysis in the form of [19]. However, in the present setting, the modulus of the wave function is not radially symmetric (nor does the DW configuration bear a complex phase structure), hence it is not directly amenable to such an approach. Understanding the origin of such an instability would consitute an interesting topic for future studies.

B. Domain-wall crosses in the rotating trap

For the rotating trap, with $\Omega_L\neq 0$ in Eqs. (7), we have found that both the symmetric and asymmetric DW crosses revolve stably in a certain frequency interval,

$$(\Omega_L)_{\min}<\Omega_L<(\Omega_L)_{\max}. \tag{16}$$

If $\Omega_L<(\Omega_L)_{\min}$, the cross does not rotate at all, while at $\Omega_L>(\Omega_L)_{\max}$ it decays (see below). These results are summarized in Fig. 3(b). In region I, the DW cross remains quiescent, in region III it gets destroyed, while the stable rotation occurs in region II. Note that there are minimum values of the trap strength which are necessary for the rotation: $\Omega_{\min}=0.012$ and 0.018 for the symmetric and asymmetric "double-vane propellers." Those values correspond to the edge points on the solid and dashed lines, respectively, in Fig. 3(b), the rotation frequencies at these points being $\Omega_L=0.0034$ and 0.010.

Note that the horizontal axis in Fig. 3(b) is extended up to a relatively large value, $\Omega=0.25$ (recall that it was assumed above that the magnetic trap's strength Ω is a small parameter, in order to derive the 2D GP equations from the underlying 3D system). According to experience accumulated in applications of asymptotic methods to various models (including the GP equation), the value 0.25 is small enough to produce reliable results.

Typical values of the physical parameters admitting the stable rotation of the DW cross can again be estimated for a mixture of two spin states in the ^{87}Rb condensate. For instance, taking the trapping frequencies $\omega_r=2\pi\times 7$ Hz and $\omega_z=2\pi\times 70$ Hz, the TF radius $R=22$ μm, and 10^3 atoms in each species, the rotation frequency $\omega_L=2\pi\times 0.84$ Hz definitely falls within the stable-rotation interval (16). Examples of a stably rotating propeller with $N_1/N_2=1.2$, and of its self-destruction in the case of $\Omega_L>(\Omega_L)_{\max}$ (for $N_1=N_2$), are shown in Figs. 5 and 6, respectively.

As it was mentioned above, a dynamical property of the DW crosses which is crucially important for their relevance to the currently available experimental settings, that have a very small value of the immiscibility parameter $|\Delta|$ [see Eq. (1)], is the fact that the crosses remain stable for all the negative values of Δ, up to $\Delta=0$. This robustness carries over to the rotating crosses, as illustrated by Fig. 7, that shows a stable rotating cross in the case of $\Delta=0$.

The results can alternatively be summarized upon considering rescaled variables in Eqs. (7) and (8). In particular, upon measuring the time, spatial variables, and normalized wave functions in units of Ω^{-1}, $\Omega^{-1/2}$, and $\Omega^{1/2}$, respectively, we obtain a system of two equations similar to Eq. (7), but with the Hamiltonian being given by

$$\hat{H}_{2D}\equiv\frac{1}{2}\nabla_\perp^2+\frac{1}{2}r^2-\frac{\Omega_L}{\Omega}L_z. \tag{17}$$

Then, we may present the domain of stability of the rotating DW crosses in the parameter plane $(N_1/N_2,\Omega_L/\Omega)$ as follows: We set $\mu_2=1$ and, for a given value of μ_1 (which sets the value of N_1/N_2), we vary the ratio Ω_L/Ω in the interval $(0,1)$. Then, we numerically integrate the system of equations for u_j, for long times, to test the stability of the rotating

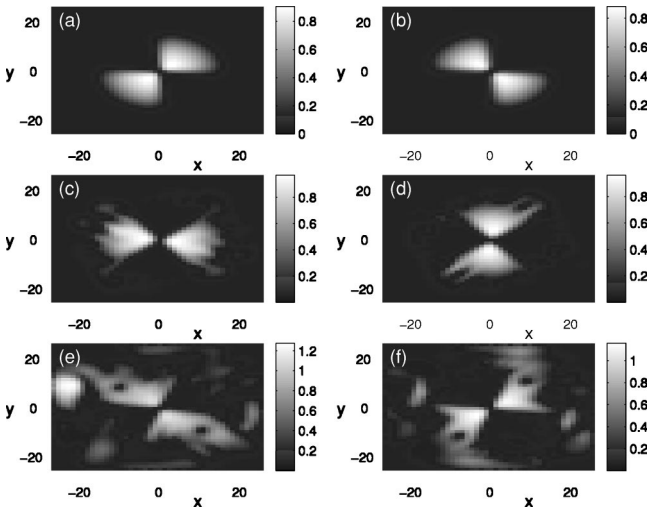

FIG. 6. An example of the evolution of an unstable symmetric "double-vane propeller" (rotating domain-wall cross). The panels in the left and right columns display the density distributions $|u_1|^2$ and $|u_2|^2$, respectively, at $t=0$ [frames (a) and (b)], $t=10$ [frames (c) and (d)], and $t=20$ [frames (e) and (f)]. The parameters are as in Figs. 2(a) and 2(b), but with $\Omega=0.1$ and $\Omega_L=0.08$.

DW cross. The results are shown in Fig. 8, where the stable-rotation region is delineated in the *full* parameter plane: In region I, the DW cross remains quiescent, in region III it is destroyed, while the stable rotation occurs in region II. Note that for values of N_1/N_2 outside the shown interval, $(0.65, 1.55)$, the DW crosses are unstable. Thus, for instance, at a typical value of the ratio between the rotation frequency and the trap strength, $\Omega_L/\Omega=0.1$, the stoichiometry ratio must belong to the interval $0.65 \leqslant N_1/N_2 \leqslant 1.55$. As mentioned above, the smallest value of Ω_L/Ω necessary for the stable rotation (which is 0.0019) corresponds to the symmetric case, $N_1/N_2=1$.

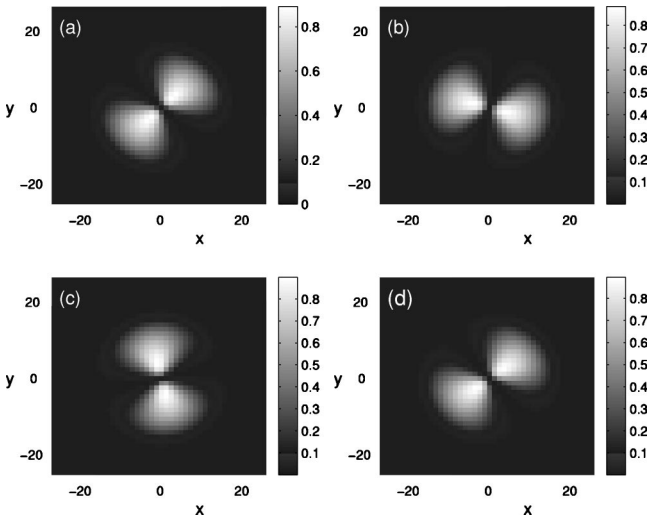

FIG. 7. A stable rotating symmetric domain-wall cross found exactly at the immiscibility border, $\Delta=0$ (corresponding to $\alpha_{11}=\alpha_{22}=\alpha_{12}=1$) and $\Omega=0.1$. The arrangement of the figure is the same as in Fig. 5.

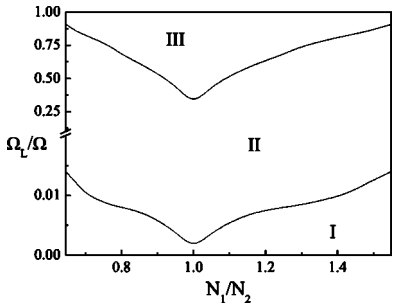

FIG. 8. The region of the stable rotation of the domain-wall crosses, shown in the parameter plane $(N_1/N_2, \Omega_L/\Omega)$. In region I, the DW cross is quiescent, in region III it is destroyed, while in region II it is rotating in a stable manner. Note that for values of N_1/N_2 outside the interval $(0.65, 1.55)$ the DW crosses are unstable.

C. More general cross and propeller patterns

All the patterns produced by the intersection of more than two DWs were found to be unstable, rearranging themselves into the fundamental crosses considered above. A typical example of that, with four intersecting DWs and $N_1/N_2=1$, is displayed in Fig. 9. The same instability of the higher-order crosses takes place in the rotating trap.

Two-dimensional patterns similar to the symmetric DW crosses can be formed in *single-component* BECs by two linear dark solitons intersecting under the right angle (provided that the dark soliton itself may be stable). We have checked that such single-component patterns are *always* unstable.

The crosses in BECs (but not in the above-mentioned photonic-crystal media) can be extended into the 3D case, as patterns formed by the intersection of planar DWs. Moreover, torque can be applied to such a structure, making it look like a double helix. Further, these patterns may revolve together with the trap. Results for the cross-shaped 3D patterns will be reported elsewhere.

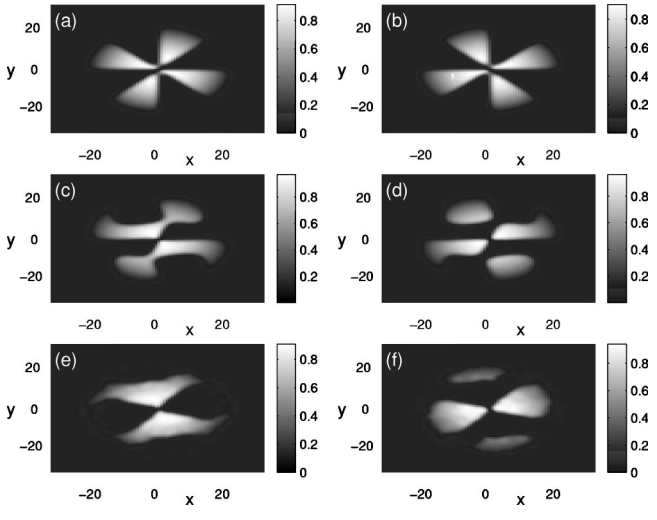

FIG. 9. Instability of a higher-order domain-wall cross (left and right panels show distributions of the densities $|u_1|^2$ and $|u_2|^2$). The frames (a) and (b) display the initial configuration at $t=0$. Further frames show the evolving configurations: (c),(d) at $t=50$, and (e),(f) at $t=600$. The parameters are as in Figs. 2(a) and 2(b).

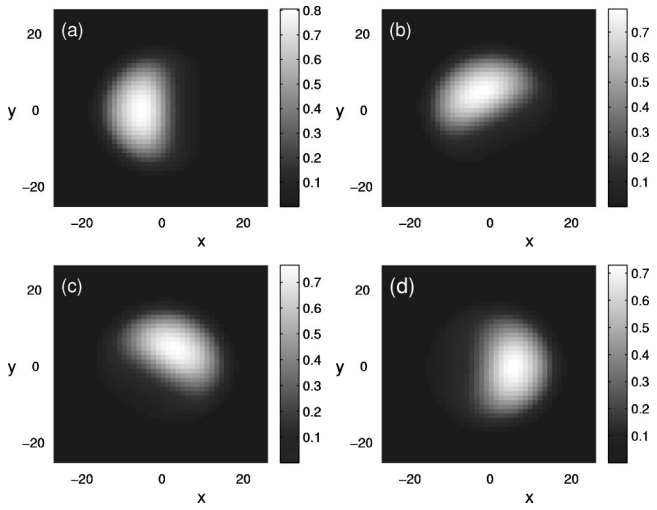

FIG. 10. Rotation of the rectilinear domain wall at the smallest value of the immiscibility parameter, $|\Delta|=0.061$ (corresponding to $\alpha_{11}=\alpha_{22}=1$, $\alpha_{12}=1.03$), and $\Omega=0.1$ at which it is stable. The arrangement of the figure is the same as in Fig. 7.

D. Rotating rectilinear domain walls

As was explained above, stable rectilinear DWs are less relevant for the currently (experimentally) tractable small values of the immiscibility parameter $|\Delta|$. Nevertheless, for completeness of the analysis, and also for the sake of possible future experiments in BEC mixtures of different atomic species, where $|\Delta|$ may be much larger than in the presently available mixtures of different spin states of the same isotope, it makes sense to briefly consider a possibility of stable rotation of the DWs of this type too. Numerical simulations show that, generally, the rectilinear DW withstands rotation, within a certain interval of the angular velocities [cf. Eq. (16)], if it is stable in the static trap. Here, we do not aim to produce comprehensive results for the stability domain of the rotating rectilinear DWs. Instead, in Fig. 10 we display an example of a stably rotating DW of this type. This example has a special purport, as it shows the rotating rectilinear DW found at the *minimum value* of the immiscibility parameters at which it may be stable, $|\Delta|=0.061$. Stable rotating rectilinear DWs found in the generic case are quite similar to the one shown in Fig. 10.

IV. CONCLUSIONS

Our analysis predicts the existence of symmetric and asymmetric domain-wall (DW) crosses in immiscible mixtures of repulsive BECs in disk-shaped traps. The stable crosses are distinguished by the phase shift of π between sectors filled by each component. The same patterns may also be carried by bimodal light beams in photonic crystal fibers (PCFs). The crosses are stable in a wide range of parameters, including a certain interval of the stoichiometry ratio N_1/N_2, the case $N_1=N_2$ being the most robust one. Adding the trap's rotation (or twist of the PCF, in the optical model), we have shown that the DW crosses can rotate, provided that the driving angular velocity (or the twist pitch, in the PCF) is limited from below and from above (if it is too small, the cross does not rotate, and if it is too large, the cross decays). In the PCF, the rotation takes place not in time, but in the spatial domain, i.e., along the propagation distance, hence the optical cross actually looks like a double helix. The rotating optical crosses have the potential for use in switching and routing applications. Full stability domains for the quiescent and rotating crosses were identified, corresponding to values of physical parameters accessible in current experiments (both for BECs and PCFs).

The crosses (including the rotating ones) persist exactly up to the zero value of the immiscibility parameter $|\Delta|$. This aspect of the robustness of the DW crosses is crucially important because, in the BEC mixtures of different spin states in ^{87}Rb and ^{23}Na, currently available to the experiment, the actual value of $|\Delta|$ is very small. We have demonstrated that, in the cases of practical interest, the simplest rectilinear (quasi-1D) DWs *do not exist* (in a stable form), while the crosses remain entirely stable. For the sake of completeness, we have also demonstrated a possibility of stable rotation of the rectilinear DWs at larger values of $|\Delta|$.

The patterns produced by the intersection of more than two DWs were observed to be unstable. They rearrange themselves into the fundamental crosses.

Finally, it is worth mentioning that, at angular velocities of the rotating trap essentially exceeding the range of values dealt with in this paper, one may expect the existence of rotating DWs separating not merely areas with the quasiuniform distribution of the densities of immiscible species, but rather areas filled with triangular vortex lattices (each species supporting its own lattice). In single-component BECs, such regular lattices, composed of a large number of vortices, have been recently studied in detail in direct experiments [20]. In fact, creation of the DW separating the vortex lattices in immiscible components is the most straightforward way for experimental observation of a *rotating* DW pattern in BECs. This possibility will be considered in detail elsewhere.

ACKNOWLEDGMENTS

We appreciate valuable discussions with L. Carr, E. Cornell, and P. Engels. B.A.M. acknowledges partial support from the Israel Science Foundation through Grant No. 8006/03, and the hospitality of JILA (Boulder, CO). P.G.K. acknowledges support from the Eppley Foundation, NSF CAREER, and NSF-DMS-0204585.

[1] M. Trippenbach, K. Goral, K. Rzazewski, B. A. Malomed, and Y. B. Band, J. Phys. B **33**, 4017 (2000);P. Öhberg and L. Santos, Phys. Rev. Lett. **86**, 2918 (2001);S. Coen and M. Haelterman, *ibid.* **87**, 140401 (2001);D. T. Son and M. A. Stephanov, Phys. Rev. A **65**, 063621 (2002);J. J. Garcia-Ripoll, V. M. Pérez-García, and F. Sols, *ibid.* **66**, 021602 (2002);B. Deconinck, J. N. Kutz, M. S. Patterson, and B. W. Warner, J. Phys. A **36**, 5431 (2003);P. G. Kevrekidis, B. A. Malomed, D. J. Frantzeskakis, and A. R. Bishop, Phys. Rev. E **67**, 036614 (2003).

[2] T. L. Ho and V. B. Shenoy, Phys. Rev. Lett. **77**, 3276 (1996);B. D. Esry, C. H. Greene, J. P. Burke Jr., and J. L. Bohn, *ibid.* **78**, 3594 (1997);P. Öhberg and S. Stenholm, Phys. Rev. A **57**, 1272 (1998);B. D. Esry and C. H. Greene, *ibid.* **59**, 1457 (1999);A. A. Svidzinsky and S. T. Chui, *ibid.* **68**, 013612 (2003).

[3] P. G. Kevrekidis, H. E. Nistazakis, D. J. Frantzeskakis, B. A. Malomed, and R. Carretero-Gonzalez, Eur. Phys. J. D **28**, 181, (2004).

[4] K. Kasamatsu, M. Tsubota, and M. Ueda, Phys. Rev. Lett. **91**, 150406 (2003).

[5] S. Ghosh, M. V. N. Murthy, and S. Sinha, Phys. Rev. A **64**, 053603 (2001).

[6] C. J. Myatt, E. A. Burt, R. W. Ghrist, E. A. Cornell, and C. E. Wieman, Phys. Rev. Lett. **78**, 586 (1997).

[7] D. S. Hall, M. R. Matthews, J. R. Ensher, C. E. Wieman, and E. A. Cornell, Phys. Rev. Lett. **81**, 1539 (1998).

[8] D. M. Stamper-Kurn, M. R. Andrews, A. P. Chikkatur, S. Inouye, H.-J. Miesner, J. Stenger, and W. Ketterle, Phys. Rev. Lett. **80**, 2027 (1998).

[9] G. Modugno, G. Ferrari, G. Roati, R. J. Brecha, A. Simoni, and M. Inguscio, Science **294**, 1320 (2001).

[10] M. Mudrich, S. Kraft, K. Singer, R. Grimm, A. Mosk, and M. Weidemuller, Phys. Rev. Lett. **88**, 253001 (2002).

[11] S. Inouye, M. R. Andrews, J. Stenger, H. J. Miesner, D. M. Stamper-Kurn, and W. Ketterle, Nature (London) **392**, 151 (1998);J. L. Roberts, N. R. Claussen, James P. Burke, Jr., Chris H. Greene, E. A. Cornell, and C. E. Wieman, Phys. Rev. Lett. **81**, 5109 (1998);J. Stenger, S. Inouye, M. R. Andrews, H.-J. Miesner, D. M. Stamper-Kurn, and W. Ketterle, *ibid.* **82**, 2422 (1999);S. L. Cornish, N. R. Claussen, J. L. Roberts, E. A. Cornell, and C. E. Wieman, *ibid.* **85**, 1795 (2000).

[12] G. Izus, M. San Miguel, and M. Santagiustina, Phys. Rev. E **64**, 056231 (2001).

[13] P. Kopperschmidt and L. C. Kimerling, Phys. Rev. B **63**, 045101 (2001).

[14] G. Kakarantzas, A. Ortigosa-Blanch, T. A. Birks, P. S. Russell, L. Farr, F. Couny, B. J. Mangan, Opt. Lett. **28**, 158 (2003).

[15] A. L. Fetter, J. Low Temp. Phys. **129**, 263 (2002).

[16] V. M. Pérez-García, H. Michinel, and H. Herrero, Phys. Rev. A **57**, 3837 (1998);Yu. S. Kivshar, T. J. Alexander, and S. K. Turitsyn, Phys. Lett. A **278**, 225 (2001);Y. B. Band, I. Towers, and B. A. Malomed, Phys. Rev. A **67**, 023602 (2003).

[17] J. J. García-Ripoll and V. M. Pérez-García, Phys. Rev. A **63**, 041603 (2001).

[18] D. L. Feder, M. S. Pindzola, L. A. Collins, B. I. Schneider, and C. W. Clark, Phys. Rev. A **62**, 053606 (2000);B. P. Anderson, P. C. Haljan, C. A. Regal, D. L. Feder, L. A. Collins, C. W. Clark, and E. A. Cornell, Phys. Rev. Lett. **86**, 2926 (2001);J. Brand and W. P. Reinhardt, Phys. Rev. A **65**, 043612 (2002).

[19] J. J. García-Ripoll, G. Molina-Terriza, V. M. Pérez-García, and L. Torner, Phys. Rev. Lett. **87**, 140403 (2001).

[20] V. Schweikhard, I. Coddington, P. Engels, V. P. Mogendorff, and E. A. Cornell, Phys. Rev. Lett. **92**, 040404 (2004).